Audio Engineering Society

Conference Paper 5

Presented at the International Conference on Acoustics & Sound Reinforcement
2024 January 23–26, Le Mans, France

Dual-Target Design for Large-Scale Sound Reinforcement: Simulation and Evaluation

Lukas Gölles[1,2] and Franz Zotter[1,2]

[1] *Institute of Electronic Music and Acoustics, 8010 Graz, Austria*
[2] *University of Music and Performing Arts Graz, 8010 Graz, Austria*

Correspondence should be addressed to Lukas Gölles (goelles@iem.at)

ABSTRACT

Progressively curved line-source arrays became state of the art in large-scale sound reinforcement as they are flexibly adapted to the listening area by well-chosen splay angles between individual elements in the chain of line-source loudspeakers. Recent perceptual studies suggest using a dual-target design to meet contradictory goals in immersive sound reinforcement: 0 dB per doubling of the distance to preserve the direct sound mix, and −3 dB per doubling of the distance to preserve the envelopment at off-center listening positions. A practical implementation has been proposed to achieve both objectives simultaneously by driving the transducers of a curved array either in phase or with individual delays. Its feasibility was verified using measurements on a miniature line array that works for small audiences, but not specifically for large arrays and audiences that would be typically found in live events. To check the applicability of the dual-target approach to large-scale sound reinforcement systems, this contribution presents a simulation study with various professional line-source arrays and a sample measurement.

1 Introduction

Providing high-quality sound for the largest parts of a predefined audience area is one of the big challenges for sound reinforcement in concerts, cinema, or speech events [1]. In the typical professional sector, large-area sound systems consider the supply with almost single-channel sound material fed to multiple line-source loudspeaker arrays. The Wavefront Sculpture Technology [2, 3] is considered a fundamental work on line array curvature design and beyond purely geometric calculation methods, Polygonal Audience Line Curving (PALC) [4, 5, 6] offers an algorithm for shaping line array contours.

As an alternative to adapting the source geometry to the listening area accordingly, beamforming-based approaches are used to obtain a desired sound level curve over the listening area, but electronically. Beamformers known from phased arrays in antenna theory, radar applications, or optics are already found in microphone arrays [7] and loudspeaker arrays [8, 9, 10]. Beamforming is typically implemented by individual delays per transducer and often with additional filtering.

Considering surround sound applications, recent research suggests a dual-target design for optimal immersive sound reinforcement, 0 dB attenuation per doubling of the distance to preserve the mixing balance of direct sound objects at off-center listening positions

[11, 12] and -3 dB per doubling of the distance to preserve the envelopment [13, 14]. Therefore, optimal immersive sound reinforcement requires a dual-target design with two individual mix buses. One contains the direct sound objects and, e.g., drives the elements of a line array in phase, assuming its curvature is designed for 0 dB per distance doubling. The other one is used for the diffuse and enveloping parts, which, e.g., require additional individual delays for each line array element to achieve -3 dB per distance doubling. Such a dual-target design was already evaluated by simulations and measurements using a miniature line array [15, 16].
To study the applicability of such a dual-target approach to professional large-scale systems, this paper presents and discusses simulations of professional line-source arrays. Simulations are done in EASE using the speaker data (.gll) provided by the manufacturers and compared to a simpler and loudspeaker-independent simulation based on point-source interference. Furthermore, the results of impulse response measurements are presented to verify the practical performance of one exemplary professional system.

2 Design of Line Array Curvature and Delay Loading (Phasing)

Considering a multi-target design, [15] presents a nonlinear differential equation that defines line array curving and phasing to achieve a $-6\cdot\beta$ dB attenuation of the direct sound,

$$\dot{\vartheta}_\mathrm{T} = -\frac{r^{2\beta}}{g^2}\frac{1}{r^2\cos\vartheta_\mathrm{w}} + \frac{\cos\vartheta_\mathrm{w}}{r} \quad \text{with } r = \frac{z}{\sin\vartheta_\mathrm{T}}\,. \tag{1}$$

g is a gain parameter and r denotes the distance for which acoustic plus electronic delay to the source is minimal, for a receiver in the xy plane. At this z coordinate of the source, ϑ_T denotes the total inclination composed of a geometric part ϑ and a delay-beamforming part ϑ_w,

$$\vartheta = a\,(\vartheta_T - \vartheta_\mathrm{offs}) + \vartheta_\mathrm{offs}, \quad \vartheta_\mathrm{w} = b\,(\vartheta_T - \vartheta_\mathrm{offs}) \quad \text{with } a+b=1\,, \tag{2}$$

where ϑ_offs is the inclination at the top coordinate $\boldsymbol{x}_0$ of the source. The convex curve geometry results from integrating over the natural length parameter s,

$$\boldsymbol{x} = \int \boldsymbol{t}\,\mathrm{d}s + \boldsymbol{x}_0\,, \qquad \boldsymbol{t} = \begin{bmatrix}\sin\vartheta & 0 & \cos\vartheta\end{bmatrix}^\mathsf{T}, \tag{3}$$

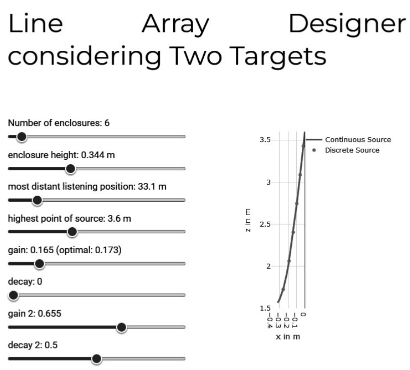

Enclosure Nr.	Tilt Angle in Degree	Observation point curved	Delays in samples @ 48 kHz	Observation point mixed
1	6.2	31.3	0	29.5
2	0.2	27.4	1	23
3	0.4	23.1	2	17.4
4	0.7	18.2	4	12.6
5	1.9	12.5	7	8.7
6	8.4	5.8	10	5.5

Print Design Sheet

Fig. 1: Line Array Designer

and the delay length $w = c\,\tau$ is calculated correspondingly,

$$w = -\int_0^s \sin\vartheta_\mathrm{w}\,\mathrm{d}s\,. \tag{4}$$

The algorithm outlined in [15, Alg.2] proposes a numerical solution of Equations 1, 3 and 4 for a mixed design of a continuous source that is discretized afterward. This algorithm is implemented in a web-based solver written in Javascript [17], cf. figure 1 that is used for line array curving and phasing in this contribution. Since this solver is capable of taking URL parameters into account, links to this tool are given in the footnote with the necessary parameters.

3 EASE and MATLAB Simulation Study

For the simulation study, we assume a listening area of 30 m depth. We use line-source arrays from different manufacturers and limit the source length to a range of 2.0 m to 2.2 m. To simulate a real-case scenario, we choose 'single motor' as rigging mode and use a single pickup point. This yields a discretization of the offset angle ϑ_offs, i.e. the inclination of the whole source. In addition, the resulting forces should also be within the permitted range, fulfilling the requirements for practical usage.

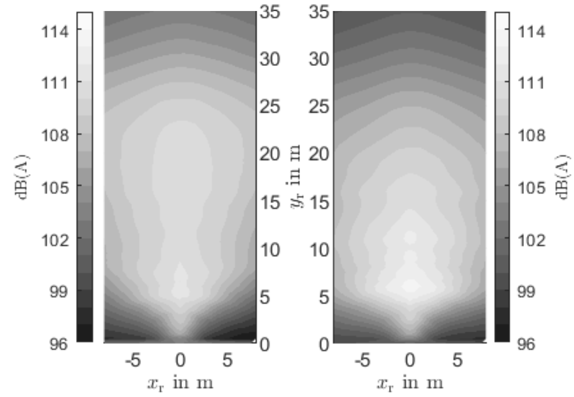

(a) Curved Design **(b)** Mixed Design

Fig. 2: GEO S12: Simulated A-weighted sound pressure over the listening area for the curved design with $\beta = 0$ and the mixed design with $\beta_2 = 0.5$ and $\beta_1 = 0$ curvature.

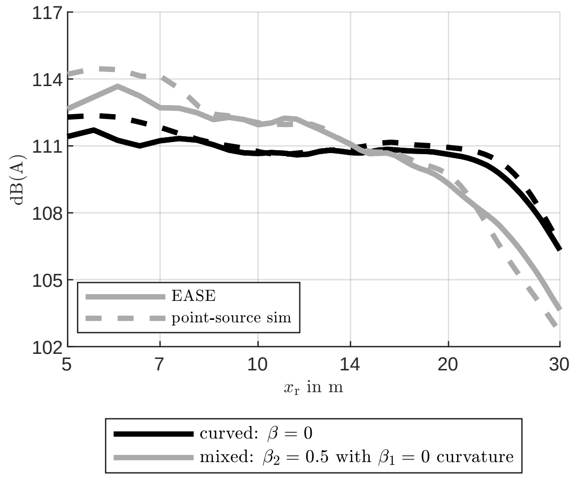

Fig. 3: GEO S12: A-weighted simulated on-axis sound pressure of curved array (black) with decay $\beta = 0$ and mixed array (grey) with $\beta_1 = 0$ and $\beta_2 = 0$ over distance compared to simulations based on point sources (dashed).

Simulations shown here are mainly done in EASE 4.4 using the corresponding speaker data provided by the manufacturers. The simulated results of the direct sound level are exported as text files to be graphically represented using MATLAB which is also used as an alternative simulation tool. To this end, the regarded line arrays are modeled as multiple point sources. These point sources are placed along the contour that is discretized into a polygon of straight-line segments with small gaps in between with the same splay-angle configurations as in EASE. The activate length around the center of each straight-line segment is simulated to get shorter by the fifth power of the frequency, i.e. for 20 Hz the length of the straight line corresponds to 90% of the discrete line-source element length and for 20 Hz it is 60%.

3.1 Nexo GEO S1210

For our requirements, six Nexo GEO S1210 elements ($N = 6$, $h = 0.344$ m) are suitable yielding a total source length of 2.06 m. The online solver[1] outputs the splay and delay parameters with farthest observation point $x_{r,0} = 33.1$ m, highest point of the source $z_0 = 3.6$ m and gain parameter $g_1 = 0.165$ for the physical curvature with design parameter $\beta_1 = 0$. For the mixed design, the second gain is $g_2 = 0.655$ to reach a -3 dB attenuation of the direct sound level when doubling the distance ($\beta_2 = 0.5$). Considering the rigging point, NS-1 predicts a negligible bumper angle error of $-0.04°$ when using pick-up position -5. Furthermore, the software reports a force on the bumper rigging point of 2.15 kN, which is well below the permitted limit of 6.8 kN. The safety factor considering all forces and moments of the entire array is 12.5.

Figure 2 presets the simulated A-weighted sound pressure over the listening area compared to a simulation based on point sources. In the majority of the listening area, the target of the curved source $\beta = 0$ is reached, cf. Figure 2a. For near observation points, we denote higher levels because the outlet of the lowest cabinet is not curved enough compared to the ideal requirement. At distant points of observation $x_r > 22$ m, there is a level drop because the stationary phase approximation assumes an infinitely extended symmetric Fresnel integral along the line source, which however only extends downwards from the top end of the line source, yielding a loss of 6 dB. Figure 2b shows the simulated level map with added delays of the mixed design. For more

[1] https://enimso.iem.sh/post/line-array-designer-two-target//?N=6&h=0.344&xr0=33.1&y0=3.6&g=0.165&beta=0&g2=0.655&beta2=0.5

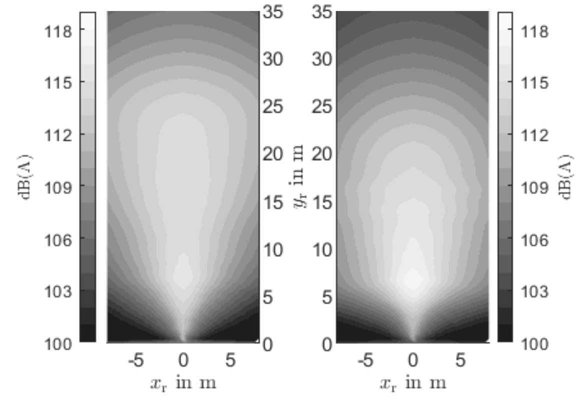

(a) Curved Design **(b)** Mixed Design

Fig. 4: KARAII: Simulated A-weighted sound pressure over the listening area for the curved design with $\beta = 0$ and the mixed design with $\beta_2 = 0.5$ and $\beta_1 = 0$ curvature.

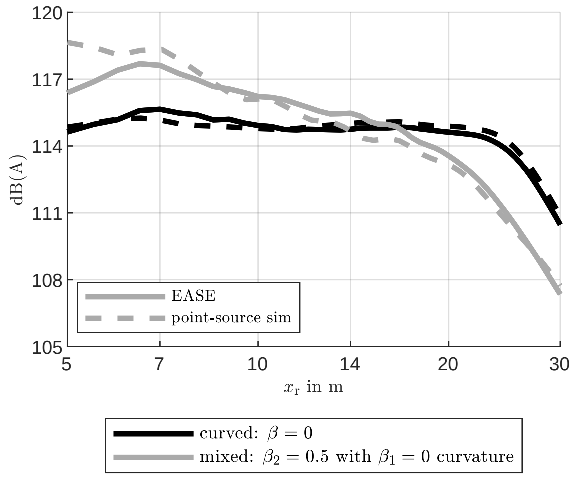

Fig. 5: KARAII: A-weighted simulated on-axis sound pressure of curved array (black) with decay $\beta = 0$ and mixed array (grey) with $\beta_1 = 0$ and $\beta_2 = 0$ over distance compared to simulations based on point sources (dashed).

detailed considerations, Figure 3 shows the on-axis level curves for both design targets. While the level stays almost constant for the $\beta = 0$ array, the results show that the target of the mixed design $\beta_2 = 0.5$ is reached when comparing the EASE simulation to the simulation based on point sources.

3.2 L'Acoustics KARAII

Next, we use eight L'Acoustics KARAII elements ($N = 8$, $h = 0.252$ m) with a total source length of 2.02 m to simulate both designs. The highest point of the source and farthest listening point remain the same as before. Due to a different source length, the gain values have to be modified[2], $g_1 = 0.165$ and $g_2 = 0.649$. The simulation in Soundvision yields a bumper error of $0.2°$ when using M-BUMP + M-BAR hole A at rigging hole 6. Although the error is small, it is taken into account in the simulations below to check the impact of this small error. Forces of 2.3 kN act at the rigging point which yields a safety factor of 11.9.

Figure 4 shows the maps of the curved design as well as the mixed design and Figure 5 presents the A-weighted direct sound curve when observing the on-axis direction. Again, the simulations show that the calculated source geometry reaches in the desired 0 dB target and that additional delays yield the desired attenuation of -3 dB per distance doubling. For both cases, we denote that the small bumper error does not have any crucial impact on the results. Furthermore, it is particularly noteworthy that the point source-based simulation mainly corresponds to the EASE simulation when considering the on-axis levels. For predicting the on-axis direct sound level, the point-source-based simulation is suitable as the deviations in more effortful EASE simulations stay reasonably low.

3.3 d&b V8

A third simulation is performed using seven d&b V8 elements ($N = 7$, $h = 0.31$ m) yielding a total source length of 2.17 m. The highest point of the source and farthest observation point remain the same as chosen for the Nexo array. Due to other enclosure dimensions, the gain values have to be modified again[3], $g_1 = 0.165$ and $g_2 = 0.655$. Using pick-up hole 19 at V flying

[2] `https://enimso.iem.sh/post/line-array-designer-two-target//?N=8&h=0.252&xr0=33.1&y0=3.6&g=0.165&beta=0&g2=0.649&beta2=0.5`

[3] `https://enimso.iem.sh/post/line-array-designer-two-target//?N=6&h=0.344&xr0=33.1&y0=3.6&g=0.165&beta=0&g2=0.655&beta2=0.5`

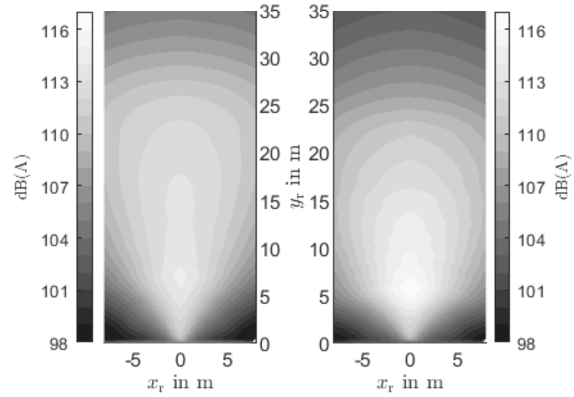

(a) Curved Design **(b)** Mixed Design

Fig. 6: V8: Simulated A-weighted sound pressure over the listening area for the curved design with $\beta = 0$ and the mixed design with $\beta_2 = 0.5$ and $\beta_1 = 0$ curvature.

frame results in a bumper error of 0.2° that is also incorporated in the simulations. ArrayCalc does not provide any information on the safety factor, only that 28 % of the load limit is reached.

Figure 6 shows the maps of the curved design as well as the mixed design and Figure 7 shows the A-weighted direct sound curve in on-axis direction. Compared to the previous results, it is noticeable that for more distant observation points lower sound pressure values are calculated in EASE for the $\beta = 0$ array than those obtained in the point source-based simulation. For the mixed array, the EASE simulation corresponds to the point-source-based simulation.

4 Measurement Study: Nexo Sample

For measurement, six Nexo GEO S1210 elements are lined up for which we calculated the source contour and simulated the direct sound levels in subsection 3.1. To record the position-dependent direct sound level curves, impulse response measurements were taken along 26 positions (on-axis) starting at $x_r = 5$ m and ending at $x_r = 30$ m. Pressure zone microphones, AKG PZM30 D, were positioned on the ground to avoid floor reflections in the measurements. We evaluated the first 300 samples of the impulse responses (6.25 ms at $f_s = 48$ kHz). Figure 8 shows the measurement setup.

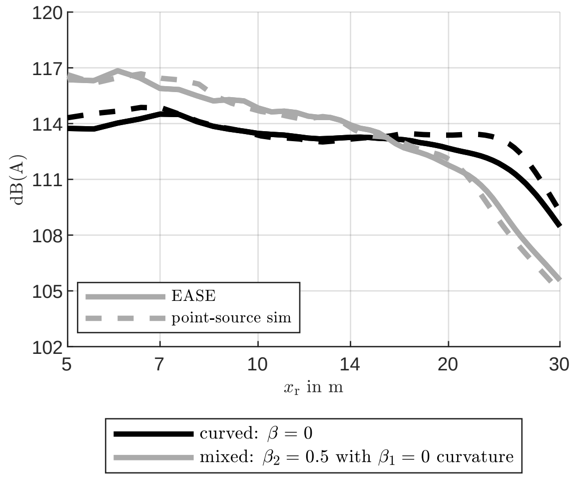

Fig. 7: V8: A-weighted simulated on-axis sound pressure of curved array (black) with decay $\beta = 0$ and mixed array (grey) with $\beta_1 = 0$ and $\beta_2 = 0$ over distance compared to simulations based on point sources (dashed).

Filter nr.	Frequency	Gain	Quality
1	386 Hz	−3.6 dB	1.004
2	539 Hz	2.7 dB	3.092
3	1203 Hz	−0.2 dB	5.738
4	3278 Hz	3.3 dB	1.417
5	8628 Hz	4.5 dB	1.118

Table 1: Filter settings for equalizing the RMS averaged response.

4.1 Equalizer

For equalization, we took the root mean squared average of the third octave averaged frequency responses of all positions. Table 1 shows the filter settings and Figure 9 presents the original averaged frequency response compared to the equalized as well as the frequency response of the proposed filter. It is noticeable that especially for higher frequency significant corrections are necessary to achieve a flat frequency response. Although it is common in practice to let the frequency response rise to low frequencies, we use a flat frequency response for broadband evaluation using A weighted sum. This makes only little difference to our analysis, as the A-filter is insensitive to low frequencies.

Fig. 8: Picture of the measurement setup: Nexo GEO S12 line-source array with pressure zone microphones on the floor.

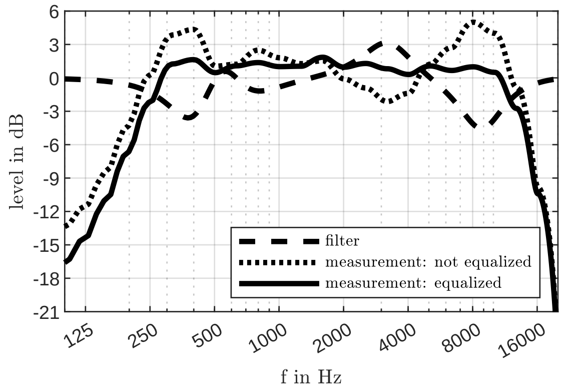

Fig. 9: GEO S12: Frequency response third octave averaged and root mean square averaged over the positions with the proposed filter.

4.2 Coverage over distance

Figure 10 shows the A-weighted on-axis sound pressure curve for the curved line-source array with $\beta = 0$ (black solid) compared to the simulation in EASE (black dotted) and the simulation of a discrete source composed of straight-line source polygons with splay angles rounded to integer degrees and leaving gaps in between the discrete elements (black dashed). For the measured level of the curved array, it sticks out that there is a boost between $x_\mathrm{r} = 7\,\mathrm{m}$ and $x_\mathrm{r} = 10\,\mathrm{m}$ and also around $x_\mathrm{r} = 20\,\mathrm{m}$. This is most likely caused by the non-flat measurement plane which sags a little and reaches the lowest point at $x_\mathrm{r} = 18\,\mathrm{m}$.
For analyzing the mixed design, the impulse response of each enclosure is shifted in time (sample-wise) as calculated by the online solver in section 3.1. Although the cabinet height of the line-source elements seems to be obstructive for the mixed design that is based on a delay and sum beamformer, the results show that the mixed design is also feasible in practice. The trend of the measured level (solid grey) coincides with the simulated one (dashed and dotted grey). The curves of both arrays were separated in the graphical representation for easier readability.

4.3 Frequency dependent radiation

Figure 11a shows the third octave averaged coverage of the $\beta = 0$ array over distance for different frequencies. To compare the results to the theoretical, Figure 11b shows the coverage of a continuous source using the point-source-based simulation. It sticks out that for low frequencies, the radiation gets point-source-like. For example, the transition radius between the far and near field is 6.2 m for 250 Hz, which is approximated by

$$r = \frac{2 f S^2}{c}, \tag{5}$$

where S denotes the source length, f the frequency and c the speed of sound [15]. For both, measurement and simulation, point-source-like radiation for all presented frequencies is seen above $x_\mathrm{r} = 18\,\mathrm{m}$ due to finite source length. It is noticeable that the mid frequencies 500 Hz and 1000 Hz are more pronounced for farther points of observation in the measurement as in the simulation. This behavior is also seen as a small deviation in Figure 12a that presents the frequency response for different points of observation. In addition to the rather flat frequency responses for the mid-frequency range for distances above 10 m, the comb filter for the response at 7 m is striking which is also visible in the results of the point source based simulation, cf. Figure 12b that is caused by different times of arrival between the enclosures of the array and the observation point. This effect is more pronounced for closer points of observation as the difference in arrival times is larger than for farther points. For frequencies above 4 kHz, the results of simulation and measurement differ because the point-source-based simulation does not incorporate behavior of the HRW (Hyperbolic Reflective Waveguide).

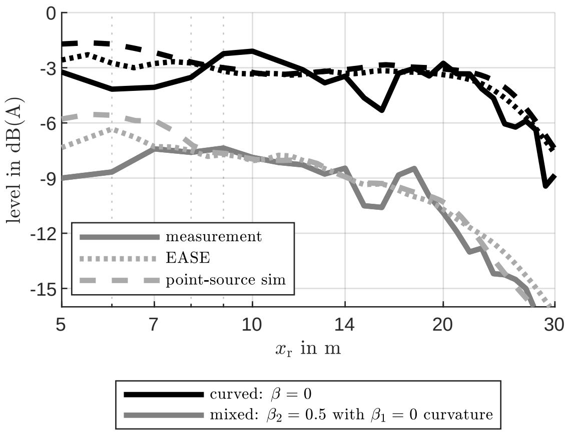

Fig. 10: GEO S12: A-weighted measured sound pressure of a curved array with decay $\beta = 0$ and mixed array with $\beta_1 = 0$ and $\beta_2 = 0$ over distance compared to simulated discretized sources.

By contrast, Figure 13a presents the third-octave averaged frequency responses of the mixed array with $\beta_2 = 0.5$ and $\beta_1 = 0$ curvature. The same filter from Figure 9 is used. The added delays lead to a position-dependent change in the impulse response of the entire array, which would require another equalization for this case, which is not implemented in our analysis. To match the frequency response of the mixed array to the response of the curved array, position-dependent filters would be necessary that are not feasible in practice. Figure 13b shows the sound level profile over distance for different frequencies of the mixed array. Compared to the purely curved array it is visible that all frequencies follow nearly the same trend. Therefore, it should be noted that design targets $\beta > 0$ are more relaxed and realistic and also more common in practical line-source array implementations.

5 Conclusion

This paper presented simulations of line-source arrays from different manufacturers considering a two-target design for immersive sound reinforcement. These showed that a mixture of curved and phased designs yields the desired targets and measurements of one system verified the simulated results in practice. Furthermore, we could show that a simplistic point-source-based simulation suitably predicts the A-weighted sum of the azimuthally on-axis direct SPL.
We plan to undertake psychoacoustic experiments using miniature line arrays surrounding the audience in medium-sized immersive sound reinforcement for 50-250 listeners. Then experiments on bigger systems using conventional line-source arrays should be conducted to implement the idea of the two-target design for larger audience areas.

6 Acknowledgment

Our research was funded by the Austrian Science Fund (FWF): P 35254-N (Envelopment in Immersive Sound Reinforcement, EnImSo). We thank Scherrer Audio Veranstaltungstechnik for their help and for letting us measure the coverage of one of their Nexo line-source arrays at their facilities in Graz.

7 Data Availability

To support reproducible research, the simulation results and the impulse responses are available in [18] for download.

References

[1] Ahnert, W. and Noy, D., *Sound Reinforcement for Audio Engineers*, Taylor & Francis Ltd, 2023, ISBN 978-1-032-11518-4.

[2] Heil, C. and Urban, M., "Sound Fields Radiated by Multiple Sound Sources Arrays," in *92nd AES Conv.*, Vienna, 1992.

[3] Urban, M., Heil, C., and Bauman, P., "Wavefront Sculpture Technology," *J. Audio Eng. Soc*, 51(10), pp. 912–932, 2003.

[4] Straube, F., Schultz, F., Makarski, M., Spors, S., and Weinzierl, S., "Evaluation Strategies for the Optimization of Line Source Arrays," in *59th AES Conf.*, Montreal, Canada, 2015.

[5] Straube, F., Schultz, F., Bonillo, D. A., and Weinzierl, S., "An Analytical Approach for Optimizing the Curving of Line Source Arrays," *J. Audio Eng. Soc*, 66(1/2), pp. 4–20, 2018.

[6] Hölter, A., Straube, F., Schultz, F., and Weinzierl, S., "Enhanced Polygonal Audience Line Curving for Line Source Arrays," in *150th AES Conv.*, 2021.

[7] Ward, D., Kennedy, R., and Williamson, R., *Microphone Arrays*, chapter Constant Directivity Beamforming, pp. 3–17, Springer Berlin, Heidelberg, 2001, ISBN 978-3-642-07547-6, doi: 10.1007/978-3-662-04619-7.

[8] Goodwin, M. and Elko, G., "Constant beamwidth beamforming," in *IEEE ICASSP*, volume 1, pp. 169–172 vol.1, Minneapolis, USA, 1993, doi: 10.1109/ICASSP.1993.319082.

[9] Meyer, D. G., "Digital Control of Loudspeaker Array Directivity," *J. Audio Eng. Soc*, 32(10), pp. 747–754, 1984.

[10] van der Werff, J., "Design and Implementation of a Sound Column with Exceptional Properties," in *96th AES Conv.*, Amsterdam, Netherlands, 1994.

[11] Gölles, L. and Zotter, F., "Optimally Curved Arc Source for Sound Reinforcement," in *Fortschritte der Akustik, DAGA*, Vienna, 2021.

[12] Zotter, F., Riedel, S., Gölles, L., and Frank, M., "Acceptable Imbalance of Sound-Object Levels for Off-Center Listeners in Immersive Sound Reinforcement," in *Fortschritte der Akustik, DAGA*, Hamburg, 2023.

[13] Riedel, S. and Zotter, F., "Surrounding line sources optimally reproduce diffuse envelopment at off-center listening positions," *JASA Express Letters*, 2(9), p. 094404, 2022, doi: 10.1121/10.0014168.

[14] Riedel, S., Gölles, L., Zotter, F., and Frank, M., "Modeling the Listening Area of Envelopment," in *Fortschritte der Akustik, DAGA*, Hamburg, 2023.

[15] Gölles, Lukas and Zotter, Franz, "Theory of continuously curved and phased line sources for sound reinforcement," *Acta Acust.*, 7, p. 52, 2023, doi: 10.1051/aacus/2023045.

[16] Gölles, L., Zotter, F., and Merkel, L., "Miniature Line Array for Immersive Sound Reinforcement," in *Proceedings of AES SIA Conf.*, Huddersfield, 2023.

[17] Lukas Gölles, "Line Array Designer considering Two Targets," https://enimso.iem.sh/post/line-array-designer-two-target/, 2023.

[18] Lukas Gölles and Franz Zotter, "Supplementary Data for Dual-Target Design for Large-Scale Sound Reinforcement: Simulation and Evaluation," https://phaidra.kug.ac.at/o:131670, 2023.

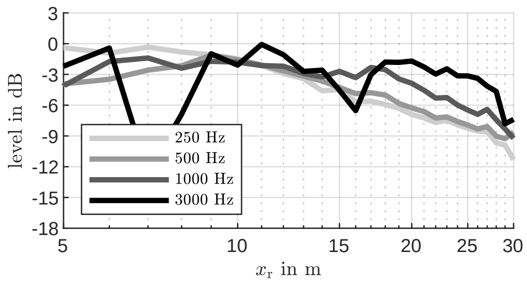

(a) Measurement.

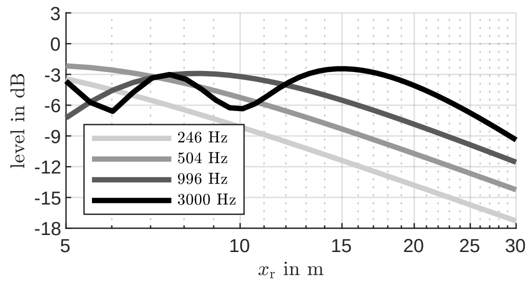

(b) Point-source-based simulation.

Fig. 11: GEO S12: Measured and simulated sound pressure of a curved array with decay $\beta = 0$ over distance for different frequencies.

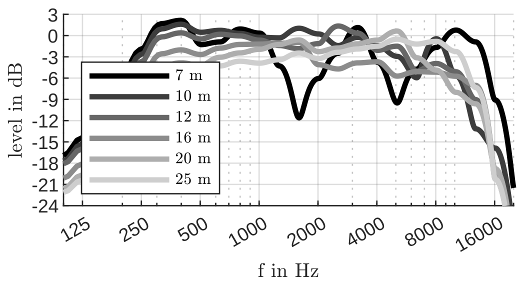

(a) Measurement.

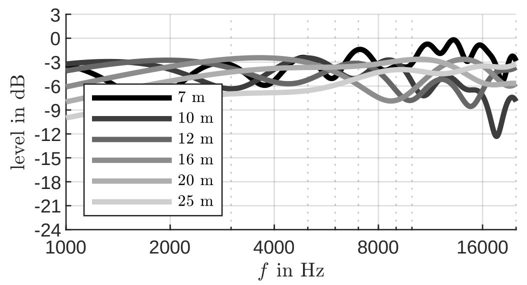

(b) Point-source-based simulation.

Fig. 12: GEO S12: Third octave averaged frequency response of $\beta = 0$ array for different positions.

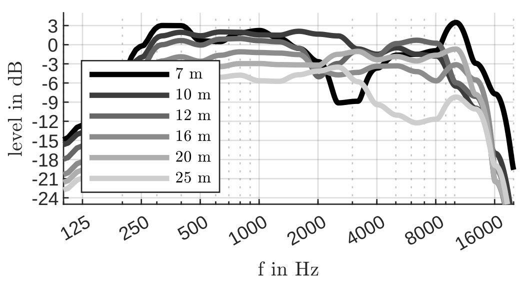

(a) Measurement.

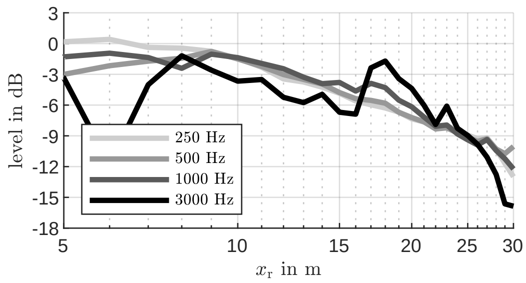

(b) Measurement.

Fig. 13: GEO S12: Third octave averaged frequency response for different positions (left) and sound pressure profile for different frequencies (right) of a mixed array with $\beta_1 = 0$ curvature and $\beta_2 = 0.5$ target.